

# Learning Self-Supervised Representations from Vision and Touch for Active Sliding Perception of Deformable Surfaces

Justin Kerr<sup>\*1</sup>, Huang Huang<sup>\*1</sup>, Albert Wilcox<sup>1</sup>, Ryan Hoque<sup>1</sup>,  
Jeffrey Ichnowski<sup>1</sup>, Roberto Calandra<sup>2</sup>, and Ken Goldberg<sup>1</sup>

**Abstract**—Humans make extensive use of vision and touch as complementary senses, with vision providing global information about the scene and touch measuring local information during manipulation without suffering from occlusions. In this work, we propose a novel framework for learning multi-task visuo-tactile representations in a self-supervised manner. We design a mechanism which enables a robot to autonomously collect spatially aligned visual and tactile data, a key property for downstream tasks. We then train visual and tactile encoders to embed these paired sensory inputs into a shared latent space using cross-modal contrastive loss. The learned representations are evaluated *without fine-tuning* on 5 perception and control tasks involving deformable surfaces: tactile classification, contact localization, anomaly detection (e.g., surgical phantom tumor palpation), tactile search from a visual query (e.g., garment feature localization under occlusion), and tactile servoing along cloth edges and cables. The learned representations achieve an 80% success rate on towel feature classification, a 73% average success rate on anomaly detection in surgical materials, a 100% average success rate on vision-guided tactile search, and 87.8% average servo distance along cables and garment seams. These results suggest the flexibility of the learned representations and pose a step toward task-agnostic visuo-tactile representation learning for robot control.

## I. INTRODUCTION

Multi-sensory cross-modal perception plays a critical role in early human cognitive development [33]. In this paper, we explore how cross-modal representations may facilitate robot perception of deformable surfaces in tasks that arise in household, medical and industrial environments such as quality inspection of garments and tumor palpation.

Prior work studies visuo-tactile representation learning in a range of applications but typically relies on significant human supervision for data collection [23, 36, 38] or learns task-specific representations [2, 4, 19, 21, 27]. While simulation can mitigate human effort, realistic tactile texture is difficult to simulate for complex objects like deformable surfaces [31]. In this work, we propose a self-supervised data collection pipeline that uses a robot with novel hardware to autonomously collect visual and tactile images that are *spatially aligned* (i.e., with a similar field of view; visual is  $2\times$  tactile). This spatial alignment allows the learned representation to capture subtle local details in appearance and texture. We use the paired data to train a visuo-tactile latent space with a cross-modal contrastive loss, a technique shown to be highly effective for vision and language representations like CLIP [28]. We decouple the texture representation from

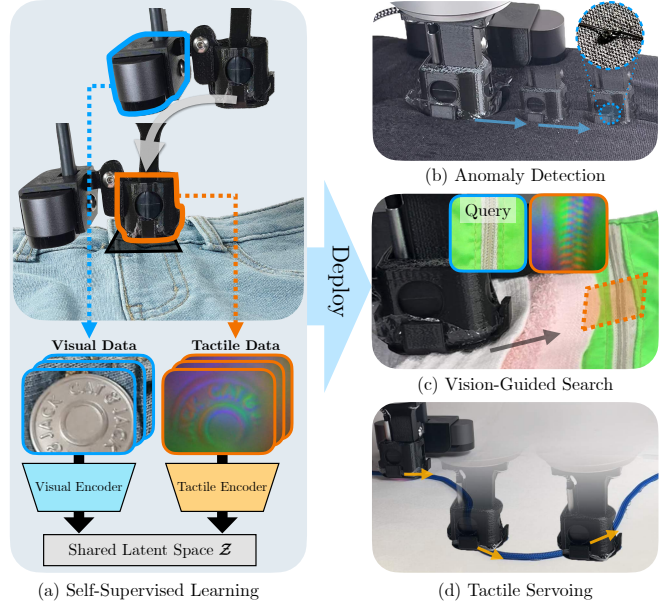


Fig. 1: **System Overview.** (a) We design a self-supervised framework described in Section IV-A to collect 4500 spatially aligned visual and tactile images, and use this dataset to learn a shared visuo-tactile latent space  $\mathcal{Z}$  as described in Section IV-B. We leverage this latent space without fine-tuning for 3 active sliding perception tasks: Anomaly Detection (b), Vision-Guided Search (c), and Tactile Servoing (d) as well as 2 passive perception tasks, classification and localization.

the rotation representation by training the latent space to be rotation-invariant and training a separate network to predict the relative rotation between a visual image and tactile image.

We show that the learned representations can be used without fine-tuning for 3 active sliding perception tasks and 2 passive perception tasks on a range of deformable surfaces, where *passive* refers to tasks that do not involve robot control (e.g., classification). We define *deformable surfaces* as 2.5-dimensional environments of area up to  $0.5\text{ m}^2$  and height up to 1 cm consisting of layers of textured deformable objects such as fabric, bags, threads, and cables. These deformable layers include varying textures (e.g., edges, corners, and seams) and embedded rigid objects (e.g., zippers, buttons, and surgical needles), but these occupy a small fraction of the workspace ( $< 10\%$ ). Figure 3 provides an example of a deformable surface environment. We define *sliding* as a 2D planar motion of the end effector with constant speed and continuous contact between the tactile sensor and a deformable surface. This sliding motion emits a stream of images with “tactile flow” [30] akin to optical flow.

<sup>\*</sup>Equal contribution.

<sup>1</sup>AUTOLab at UC Berkeley

<sup>2</sup>Meta AI

An overview of the proposed system is presented in Figure 1. This paper makes the following contributions:

- 1) A novel framework and hardware design for self-supervised real data collection collecting spatially aligned visual and tactile images pairs on deformable surfaces.
- 2) A representation learning method decoupling texture and rotation by training a rotation-invariant latent space using contrastive loss and a separate network to predict differences in rotation.
- 3) Methods using the learned representations for 3 sliding perception tasks: tactile anomaly detection, vision-guided search, and active tactile servoing, and 2 passive tasks: localization and classification.
- 4) A publicly available visuo-tactile dataset with 4500 samples of real-world, spatially aligned visual and tactile samples on deformable surfaces, in contrast to prior large datasets without such spatial alignment.

Experimental results suggest the learned visuo-tactile representation’s flexibility, motivating future investigation of broader task-agnostic representations for robot manipulation.

## II. RELATED WORK

### A. Tactile Sensing for Robotics

Tactile sensing is a longstanding challenge in robotics, with early work in active sensing based on sensor kinematics and active exploration [11]. There are various tactile sensors with different sensing techniques, resolutions, and form factors such as force-torque sensors [5, 7], haptic devices [3, 26], and soft “E-skin” that mimics human skin [25]. New sensors widely used in the past few years are the DIGIT [16] and the GelSight [10]. These sensors illuminate a flexible membrane with colored LED light from different directions and observe the back of the membrane with a camera. When materials are pressed into the membrane, their indentations are illuminated and the resulting texture forms an image.

Tactile sensing is of renewed interest for robotic learning and manipulation. Reinforcement learning (RL) policies trained with tactile information can generalize to new object geometries for insertion tasks [9]. Lu *et al.* [22] develop a tactile based SLAM method to reconstruct object geometries. Object pose estimation also benefits from tactile information [1] and can be applied to manipulation tasks such as bottle opening [14]. She *et al.* [32] learn to follow cables with tactile sensing and control. Tactile information generation in simulation has been studied [12] and can be used with RL for zero-shot sim-to-real transfer to manipulation tasks [6]. Sunil *et al.* [34] and Suresh *et al.* [35] incorporate tactile sliding for cloth unfolding and touch localization on known object geometries, respectively. In this work, we learn a visuo-tactile association from real data and apply it to three robot sliding perception tasks without fine-tuning.

### B. Visuo-Tactile Cross-modal Learning

Building a connection between tactile and visual inputs has been studied in the context of lifelong learning [40] and synthesizing sensory inputs from their counterparts [20, 36]. Takahashi *et al.* [36] use a low-resolution 16×16 grid

of pressure sensing “taxels,” and train an encoder-decoder structure to predict taxel values based on input images of a material’s texture. Lee *et al.* [18] and Li *et al.* [20] use video frames to synthesize outputs of a GelSight tactile sensor given a visual image of a robot touching a surface and vice versa using a conditional Generative Adversarial Network (cGAN) architecture. Recent work uses a cGAN conditioned on the output of a neural radiance field [24] to synthesize tactile images [41]. In contrast, the goal of this paper is not to synthesize tactile images from vision input but instead learn a shared representation from real vision and tactile sensor data for application to robot perception and control.

Yuan *et al.* [38] learn an embedding space by jointly training CNNs for three modalities: RGB images, depth images, and tactile images; they use the distance in the embedding space to match among modalities and apply their methods to infer tactile properties of fabric from vision. Similarly, Luo *et al.* [23] propose a fusion method to associate tactile and vision data of fabrics by applying maximum covariance analysis for the latent vectors. Zambelli *et al.* [39] study several approaches for cross-modal learning of vision and touch from self-supervised data. However, these papers do not explicitly apply their representations to robot control tasks. Additionally, the visual and tactile images we use in this work are spatially aligned while most visual inputs in prior work have a field of view orders of magnitude larger than the tactile images, making it difficult for networks to learn or actively perceive subtleties in local texture like edges and wrinkles that are critical for manipulation.

## III. PROBLEM STATEMENT

We consider the problem of learning a cross-modal representation between vision and tactile data that can be applied to different robot visuo-tactile perception tasks on deformable surfaces without fine-tuning. Given a robot with a tactile sensor and RGB camera attached to its end effector and a set of deformable surfaces, the goal is to output a function  $f : O_{\text{vis}} \times O_{\text{tac}} \rightarrow \mathcal{Z}$  where  $O_{\text{vis}} = \mathbb{R}^{H \times W}$  and  $O_{\text{tac}} = \mathbb{R}^{H \times W \times 3}$  are the input spaces of grayscale visual images and tactile images respectively, and  $\mathcal{Z}$  is an arbitrary output representation space. We make the following assumptions:

- 1) Objects in deformable surface environments are 1-dimensional or 2-dimensional deformable objects (e.g., cables, threads, towels, and garments).
- 2) Objects in deformable surface environments are placed on a flat tabletop in stable poses.
- 3) Deformable surfaces in downstream tasks are within the training distribution of the representation space.

During evaluation, we keep  $f$  constant across tasks and evaluate by measuring the performance of policies leveraging  $f$  on five perception tasks on deformable surfaces:

- 1) *Tactile Anomaly Detection* (Active Sliding): Given a stream of tactile readings during a sliding motion (see Section IV-D), the task objective is to localize where a tactile anomaly  $X$  occurs (e.g., a knot in an otherwise

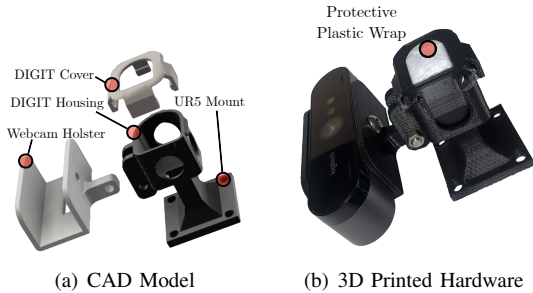


Fig. 2: **Custom Hardware Design:** (a) A CAD model of the mechanical mount designed for data collection with the RGB camera and tactile sensor. (b) The actual sensors and the mount.

untangled thread). A trial is successful if the robot stops while touching  $X$ .

- 2) *Vision-Guided Search* (Active Sliding): Given a visual query image, the task objective is to search the workspace with the tactile sensor to find a match. A trial is successful if the robot stops while touching the feature contained in the query image.
- 3) *Tactile Servoing* (Active Sliding): Given a reference visual image of a uniform directional feature (e.g., cable or towel edge), and a line in the image frame specifying which direction to slide in, the objective is to servo the tactile sensor along the feature without losing contact. We measure the distance followed without losing continuous contact between the sensor and feature.
- 4) *Tactile Classification* (Passive): Given a tactile query image and a set of canonical visual images (one image per class), the task objective is to determine which class the tactile image corresponds to.
- 5) *Tactile Localization* (Passive): Given a tactile query image and a visual observation of the entire 2D workspace, the task objective is to localize in the visual image where the tactile reading was taken.

#### IV. METHODS

We collect self-supervised data using custom hardware (Section IV-A). The collected dataset is used to train both the encoders (Section IV-B) and the rotation network (Section IV-C). These networks are then used in active sliding perception primitives (Section IV-D) and passive perception modules (Section IV-E) for five downstream tasks.

##### A. Self-supervised Data Collection Procedure

We design a self-supervised data collection pipeline in real that uses a robot to collect paired tactile and vision images on the deformable surfaces defined in Section III. We design a custom end-effector (Figure 2) to hold both sensors parallel to each other with a fixed offset  $d$  between the camera and tactile sensor. The mount includes a thin layer of protective plastic wrap over the sensor, which improves implementation of a *sliding* primitive for deformable surfaces that mitigates friction (Section I). Unlike many prior works that train on images with a large field of view, we zoom in closely when collecting visual images so that their field of view is similar

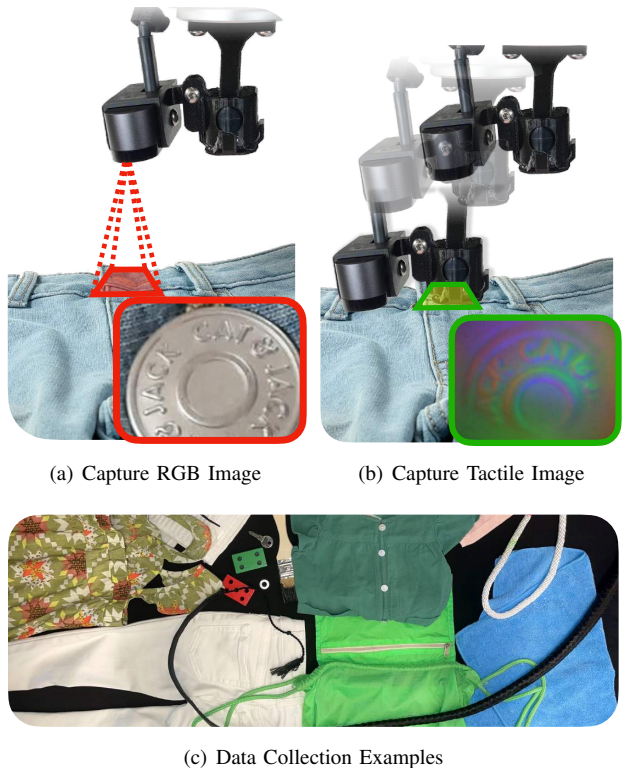


Fig. 3: **Self-Supervised Visuo-Tactile Data Collection:** An overview of the data collection pipeline. (a) For each sample the robot first uses an RGB camera to take a closely cropped image of the texture. (b) The robot then adjusts its end effector to take a tactile reading at the same location. (c) We collect data on 10 deformable surface environments, one of which is shown here.

to the tactile images (roughly  $2\times$  larger), allowing the visual images to show detailed local textures. At the beginning of each round of data collection, a human sets up the workspace by laying out 5-15 different objects at stable poses on a flat surface to form a deformable surface (see Section III). The robot then samples planar translations on a predefined grid covering the workspace with grid lines separated by 2 cm and a fixed height offset above the surface. For each sample, we generate random noise uniformly between  $-2$  cm and 2 cm in translation and between  $0^\circ$  and  $45^\circ$  in rotation to mitigate aliasing induced by grid sampling. The robot moves to the noisy translation, takes an visual image using the camera, moves the constant  $d$  offset along the horizontal direction, moves down until the contact force reaches a predefined threshold, and takes the reading from the tactile sensor. Thus, the collected tactile and vision images are automatically spatially aligned with similar field of view. The pipeline takes 11 samples per minute, with minimal human involvement required to periodically reset the surface with new objects. This pipeline is shown in Figure 3.

##### B. Encoder Training

We train a vision encoder  $f_\theta : O_{\text{vis}} \rightarrow \mathcal{Z}$  and a tactile encoder  $g_\phi : O_{\text{tac}} \rightarrow \mathcal{Z}$ , where  $\mathcal{Z} = \{z \in \mathbb{R}^d : \|z\| = 1\}$  is a shared output representation space with  $d \ll H \times W \times 3$ . We use the collected data (Section IV-A) and a contrastive

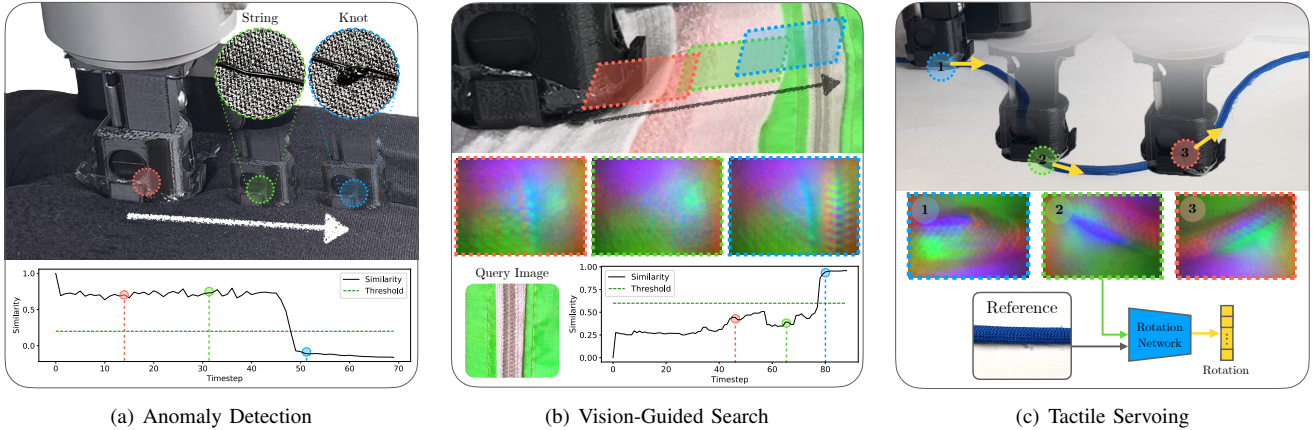


Fig. 4: **Active Sliding Perception Tasks.** (a) Anomaly Detection: The robot uses the learned tactile encoder to detect a knot while sliding over a black thread on a black surface. (b) Vision-Guided Search: Here the system is given a query visual image of a zipper and searches the workspace for a tactile reading that is sufficiently similar to the query (i.e., the texture of a zipper). (c) Tactile Servoing: The robot uses rotation predictions to follow a curved cable.

loss to learn a visuo-tactile association in a latent space. We use grayscale camera images as input to the visual encoder to avoid overfitting to colors of materials, and we augment all images with flips and color jitter of brightness and contrast to make the network less sensitive to input image orientation and lighting. For each visuo-tactile image pair we also apply random rotation uniformly between  $0^\circ$  and  $360^\circ$  to the tactile images to encourage rotation-invariant learning. During training we apply InfoNCE loss to the pairwise dot products of the embedding vectors, which intuitively pushes the correct pair of visuo-tactile readings together and all others apart. We constrain embedding vectors to have unit length, as in other contrastive learning work [28]. The final loss is then  $L_{\text{contrastive}} = \text{cross\_entropy}(I_e \times T_e^T, [0 \dots B])$ , where  $T_e$  and  $I_e$  are batched embeddings of the tactile and visual images respectively and  $B$  is the batch size. The outputs of the trained encoders are  $d$ -dimensional embeddings in the learned latent space.

### C. Rotation Prediction Network

We train a separate rotation network  $h_\psi : O_{\text{vis}} \times O_{\text{tac}} \rightarrow [0, 1]^{N_b}$  on the same dataset to learn the difference in rotation between a vision image and a tactile image (rotated via data augmentation). We use color augmentation to prevent potential spurious lighting statistics in the data [8]. We discretize the rotations into  $N_b$  buckets uniformly between  $0^\circ$  and  $360^\circ$  and formulate the problem as classification where the input is a concatenated visuo-tactile image pair and the output is a distribution over bucket indices.

### D. Active Sliding Perception Primitives

We implement three active sliding perception primitives for use in downstream tasks (Figure 4) using the trained encoders and rotation network without fine-tuning.

1) *Tactile Anomaly Detection*: To inspect garments and other objects, humans often slide their hands across the surface to detect imperfections. We mimic this behavior by sliding the tactile sensor across a deformable surface and

using the trained tactile encoder to localize tactile anomalies in materials. The system takes tactile readings while sliding and encodes them with  $g_\phi$ . The system maintains a sliding window  $\mathcal{B}_h$  containing past tactile embeddings and continually evaluates the median cosine similarity between the current embedding and the embeddings in the window. If the median similarity crosses a predefined threshold  $m_1$ , the system outputs that it has detected an anomaly candidate and slows the robot down to take  $n_1$  more readings. If the median similarity remains below  $m_1$ , the system outputs an anomaly; otherwise, the system resumes sliding at the original speed.

2) *Vision-Guided Search*: When searching for a specific tactile feature in a deformable surface (e.g., a button in a shirt), anomaly detection is insufficient due to the existence of distractors. To remedy this, we search for a visual query image. The primitive is parameterized by a visual image of the target location, which is embedded into the shared latent space. While sliding, the system computes the cosine similarity between the current tactile embedding and the query image embedding. If the similarity is above  $m_2$ , the policy slows down the robot to takes  $n_2$  more tactile readings. If the median similarity remains greater than  $m_2$ , the system outputs that it has found the target; otherwise, it resumes sliding at the original speed.

3) *Tactile Servoing*: Another useful primitive for tactile manipulation is actively servoing along material features like edges, cables and seams. Prior approaches utilize analytic methods [32] or supervised learning with human labels [34]. In our work, we use the pretrained rotation network to servo given an input visual query image, which specifies the feature to follow as well as the direction. The system uses the rotation network to predict the rotation  $R_t$  between the query visual image and the current tactile image. It approximates network confidence as the variance of the prediction distribution. To estimate a feature-centering offset, the system translates the visual reference orthogonally to the rotation prediction in a grid search to maximize prediction confidence and chooses the direction corresponding to high-

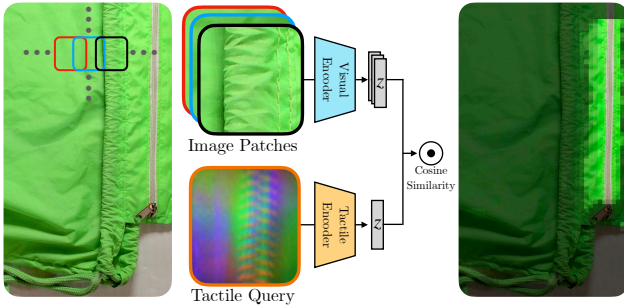


Fig. 5: **Tactile Localization:** An input tactile image of the zipper is compared to discretized patches from a visual image of the entire scene. In this example, the heatmap shows high probability of a match near the zipper.

est confidence as the translation direction  $T_t$ .

### E. Passive Perception Modules

We develop two modules that use the encoders without fine-tuning for passive tactile perception: a localizer module for localization and a classifier module for classification.

1) *Tactile Localizer:* Given a top-down visual image of the entire workspace and a tactile image, this module outputs a probability distribution over possible contact locations. We divide the input visual image into a grid with uniform patch size and resolution and compute cosine similarity of each patch embedding with the tactile embedding as shown in Figure 5. This produces a distribution over patch locations of the predicted similarity between vision and touch.

2) *Tactile Classifier:* Classification of features in input tactile images (e.g., distinguishing between towel edges and corners) is a common task. Prior work performs tactile classification with supervised learning [34], but human supervision is time-consuming. Instead, we construct a classifier from trained encoders by providing canonical visual images of the classes we consider. We augment these visual images with the same augmentation as performed during training and embed them into  $\mathcal{Z}$ . We use the weighted  $k$ -nearest neighbors algorithm to classify the tactile input (Figure 6), a technique shown to be effective in classification with latent spaces [37].

## V. PHYSICAL EXPERIMENTS

We assess the utility of the learned representations on 3 active sliding perception tasks and 2 passive perception tasks. Throughout all experiments, the same trained networks are used without fine-tuning to evaluate the generality of the learned representations.

We collect self-supervised data (Section IV-A) with a UR5 robot arm, a DIGIT tactile sensor [16], and a Logitech BRIO webcam. The data consist of 4500 visuo-tactile pairs over 10 deformable surface environments collected over 7 hours of robot-time. We train a texture latent space (Section IV-B) with an embedding dimension of  $d = 8$ , obtained via grid search over  $d \in [8, 16, 32, 64]$ . We optimize using Adam [15] with default parameters and a batch size of  $B = 512$ . We train the rotation network (Section IV-C) with a batch size of  $B = 32$ ,  $N_b = 18$ , and Cross Entropy Loss. All networks use a RegNetY\_800MF backbone [13] because of its optimization

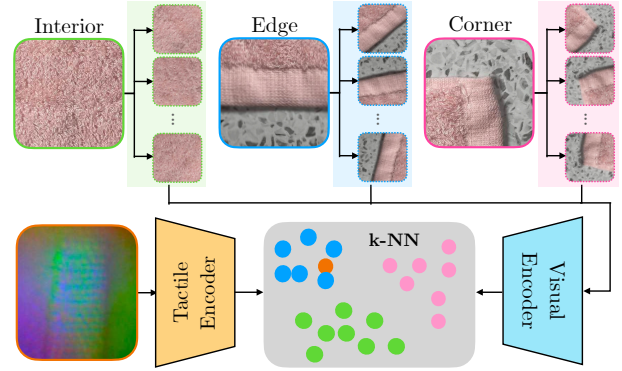


Fig. 6: **Tactile Classification** Given canonical visual images of categories (images in solid line), we augment these inputs (images in dashed line) and embed them into the latent space, then apply  $k$ -NN classification on tactile input images.

for performance per MFLOP. We initialize all networks with weights pretrained on ImageNet [29] classification.

### A. Active Sliding Tasks

For these tasks, the experiment starts with the robot pushing down at the given start position until a force of 20 N is reached. The robot slides at a speed of 1 cm/s along the predefined path acquiring the tactile readings at a rate of 10 Hz. All the experiments below are conducted without vision input other than the query and reference vision images to mimic occlusions in practice.

1) *Tactile Anomaly Detection:* For this experiment we set  $|\mathcal{B}_h| = 40$ ,  $m_1 = 0.3$ , and  $n_1 = 20$ . The robot is slowed to 20% speed when an anomaly candidate is detected. A trial is considered successful if the robot stops at a tactile reading that contains the anomaly. Each experiment consists of 10 trials with varying start locations. Figure 4(a) shows an example. As a baseline, we apply the same buffer and active confirmation technique but using a threshold on the L2 pixel distance between tactile images over time. We consider the following 2 settings: **Knot detection on surgical thread:** We fix a 1 mm black surgical thread on top of black cloth (difficult to visually perceive) and tie a knot anomaly to detect. We conduct experiments on a 1 mm knot and a 3 mm knot respectively. **Tumor palpation:** To simulate the stiffness of a tumor embedded in flesh, we embed a 3 mm hex nut in soft foam, 1 cm beneath the surface. Table I results suggest that the policy with the trained encoders achieve an average 73% success rate on the three settings, while the baseline achieves an average 37% success rate. The baseline performance drops significantly on the smaller knot, suggesting it's sensitive to the anomalies size, while our policy achieve similar success rates on both knots. Both policies achieve low success rates on the tumor detection due to the more subtle changes in the tactile readings.

2) *Vision-Guided Search:* In these experiments, to test if Vision-Guided Search can differentiate targets from multiple distractors, we include false tactile anomalies along the path of the robot to the correct feature. We use  $m_2 = 0.6$  and

TABLE I: Anomaly detection success rate.

Algorithm	Knot 3mm	Knot 1mm	Tumor
Baseline	9/10	0/10	2/10
Our method	9/10	8/10	5/10

TABLE II: Vision-guided search success rate.

Algorithm	Zipper	Garment	Button
Baseline	0/10	1/10	5/10
Our method	10/10	10/10	10/10

TABLE III: Tactile servoing distance % completed.

Algorithm	S-Shaped Cable	Dress Seam	Shirt Seam
Baseline	12.7 $\pm$ 24.0	43.1 $\pm$ 35.4	18.8 $\pm$ 9.6
Our method	<b>78.7 <math>\pm</math> 3.4</b>	<b>92.2 <math>\pm</math> 23.3</b>	<b>92.4 <math>\pm</math> 19.1</b>

TABLE IV: Classification results on towel edges, corners, and interiors. We use K-nearest neighbor classification on the latent embeddings of a small set of canonical *visual* images to classify new *tactile* images (Sec. IV-E.2). N refers to the number of datapoints, and “primary confusor” is the mode of mis-classifications.

Category	Accuracy (%)	Primary Confusor	N
Edge	75	Corner	36
Corner	93	Edge	30
Interior	74	Edge	43
Overall	80	N/A	109

$n_2 = 60$ . The robot is slowed to 20% speed when a target candidate is detected. Figure 4(b) shows an example. We use Tactile Anomaly Detection as a baseline, and run 10 trials for each experiment varying the start location. An experiment is a success if the robot stops with the feature specified by the visual image in the tactile image. We consider the following three settings: **Multi-texture garment**: The robot searches for a ruffled portion of a dress amidst seams and crumples, a subtle difference in tactile texture to detect. **Finding a zipper among multiple edges**: The robot searches for a zipper on a multi-textured surface. We layer two different towels on a bag with a zipper, and the query image is a visual image of the zipper (Figure 4(b)). **Finding a button in a blouse**: The robot slides on a blouse until a button is found, ignoring seams along the way.

The results summarized in Table II show that our policy achieves 100% success rate while the baseline achieves 20% average success rate, suggesting that the learned latent space can successfully correlate the tactile and vision information.

3) *Tactile Servoing*: For each experiment, the input is a visual image of a horizontal segment of the feature. We smooth  $R_t$  by  $\hat{R}_t = \lambda R_t + (1 - \lambda)R_{t-1}$ , where  $\lambda = 0.8$  is chosen empirically. This results in the overall sliding direction of  $\hat{R}_t + T_t$ . We measure the distance successfully traveled by the robot without losing contact. As a baseline, we use the contact ellipse estimation from PyTouch [17] to obtain a rotation direction to move. We conduct 10 trials at the same start location. We conduct the experiments on a 2 mm diameter, 30 cm length **S-shaped cable** fixed on the work surface, a **dress seam** in the middle of a dress with wrinkles on the side and a **shirt seam** near a shirt collar.

The percent distance traveled is in Table III. While the

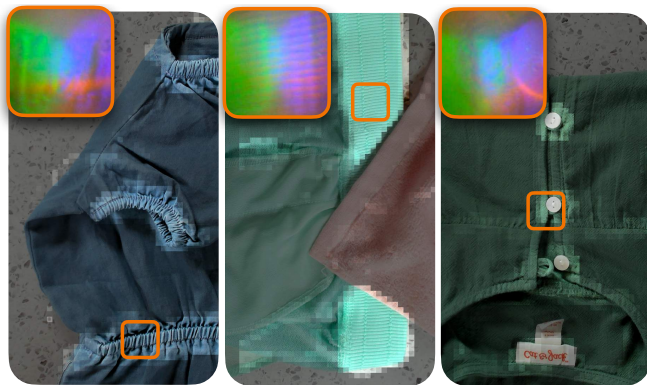


Fig. 7: **Localization Visualizations**: We show 3 illustrative contact localization results; a wrinkled dress seam, an elastic band, and blouse buttons. The heatmaps are composited onto the original image by scaling them between  $[0, 1]$ , applying gamma correction  $\gamma = 1.6$ , and multiplying them by the value channel. Orange boxes denote the location of the tactile query.

baseline travels up to 43.1% of the total distance, our policy travels at least 78.7% of the total distance. The baseline is sensitive to textures that confuse the ellipse fitting, while our rotation network prediction is robust to local textures and focuses on the global spatial relations. The major failure cases of our network are the ambiguity in the servoing direction and the errors from  $T_t$ .

## B. Passive Perception

1) *Tactile Localization*: Since many locations in the visual image may generate nearly identical tactile readings, such as the interior of a fabric, we provide qualitative visualizations of localization heatmaps in Figure 7. Similar textures as the ground truth touch location are smoothly activated, suggesting the encoder has learned a mapping between visual and tactile appearance rather than overfitting to specific locations.

2) *Tactile Classification*: We manually collect a dataset of 109 tactile images of corners, edges, and interiors of 2 different towels, and use 4 canonical visual images per category to instantiate the K-NN classifier. We use 100 augmentations of the 4 canonical images to smooth decision boundaries and  $k=50$ . Results are shown in Table IV. We hypothesize that the edges are occasionally confused as corners because they look locally similar, while the interiors are misclassified as edges due to the similarity in texture of one towel interior to the other’s edge.

## VI. DISCUSSION

In this paper, we propose a framework for learning visuo-tactile representations from self-supervised data and apply the learned representations to 3 active and 2 passive perception tasks. Results suggest the flexibility of the learned representation for multi-task usability.

The approach has a few limitations. The learned latent space is non-metric, making performance on query tasks sensitive to the chosen threshold. In addition, the distribution of objects is limited to 2.5-dimensional deformable surfaces with the DIGIT sensor on the table, though we hypothesize that similar manipulation policies can be constructed for in-hand sliding as well. Lastly, some human supervision is still

required to reset the scene between rounds of data collection; fully automating the data collection procedure would greatly improve the scalability of the method.

#### REFERENCES

- [1] M. Bauza, A. Bronars, and A. Rodriguez, “Tac2pose: Tactile object pose estimation from the first touch,” *arXiv preprint arXiv:2204.11701*, 2022.
- [2] M. Bauzá, O. Canal, and A. Rodriguez, “Tactile mapping and localization from high-resolution tactile imprints,” *2019 International Conference on Robotics and Automation (ICRA)*, pp. 3811–3817, 2019.
- [3] M. A. Cabrera, O. Sautenkov, J. Tirado, A. Fedoseev, P. Kopanov, H. Kajimoto, and D. Tsetserukou, “Deepxpalm: Tilt and position rendering using palm-worn haptic display and cnn-based tactile pattern recognition,” in *2022 IEEE Haptics Symposium (HAPTICS)*, 2022, pp. 1–6.
- [4] R. Calandra, A. Owens, D. Jayaraman, J. Lin, W. Yuan, J. Malik, E. H. Adelson, and S. Levine, “More than a feeling: Learning to grasp and regrasp using vision and touch,” *IEEE Robotics and Automation Letters*, vol. 3, no. 4, pp. 3300–3307, Oct. 2018.
- [5] M. Y. Cao, S. Laws, and F. R. y. Baena, “Six-axis force/torque sensors for robotics applications: A review,” *IEEE Sensors Journal*, vol. 21, no. 24, pp. 27 238–27 251, 2021.
- [6] A. Church, J. Lloyd, N. F. Lepora, *et al.*, “Tactile sim-to-real policy transfer via real-to-sim image translation,” in *Conference on Robot Learning*, PMLR, 2022, pp. 1645–1654.
- [7] M. R. Cutkosky, R. D. Howe, and W. R. Provancher, “Force and tactile sensors,” in *Springer Handbook of Robotics*, B. Siciliano and O. Khatib, Eds. Berlin, Heidelberg: Springer Berlin Heidelberg, 2008, pp. 455–476.
- [8] C. Doersch, A. K. Gupta, and A. A. Efros, “Unsupervised visual representation learning by context prediction,” *2015 IEEE International Conference on Computer Vision (ICCV)*, pp. 1422–1430, 2015.
- [9] S. Dong, D. K. Jha, D. Romeres, S. Kim, D. Nikovski, and A. Rodriguez, “Tactile-rl for insertion: Generalization to objects of unknown geometry,” in *2021 IEEE International Conference on Robotics and Automation (ICRA)*, IEEE, 2021, pp. 6437–6443.
- [10] S. Dong, W. Yuan, and E. H. Adelson, “Improved GelSight tactile sensor for measuring geometry and slip,” in *2017 IEEE/RSJ International Conference on Intelligent Robots and Systems (IROS)*, IEEE, Sep. 2017.
- [11] K. Goldberg and R. Bajcsy, “Active touch and robot perception,” *Cognition and Brain Theory*, vol. 7, no. 2, pp. 199–214, 1984.
- [12] D. F. Gomes, P. Paoletti, and S. Luo, “Generation of gelsight tactile images for sim2real learning,” *IEEE Robotics and Automation Letters*, vol. 6, no. 2, pp. 4177–4184, 2021.
- [13] K. He, X. Zhang, S. Ren, and J. Sun, “Deep residual learning for image recognition,” *2016 IEEE Conference on Computer Vision and Pattern Recognition (CVPR)*, pp. 770–778, 2016.
- [14] T. Kelestemur, R. Platt, and T. Padir, “Tactile pose estimation and policy learning for unknown object manipulation,” *arXiv preprint arXiv:2203.10685*, 2022.
- [15] D. P. Kingma and J. Ba, “Adam: A method for stochastic optimization,” *International Conference for Learning Representations*, vol. abs/1412.6980, 2015.
- [16] M. Lambeta, P.-W. Chou, S. Tian, B. Yang, B. Maloon, V. R. Most, D. Stroud, R. Santos, A. Byagowi, G. Kammerer, D. Jayaraman, and R. Calandra, “DIGIT: A novel design for a low-cost compact high-resolution tactile sensor with application to in-hand manipulation,” *IEEE Robotics and Automation Letters*, vol. 5, no. 3, pp. 3838–3845, Jul. 2020.
- [17] M. Lambeta, H. Xu, J. Xu, P. Chou, S. Wang, T. Darrell, and R. Calandra, “Pytouch: A machine learning library for touch processing,” *CoRR*, vol. abs/2105.12791, 2021. arXiv: 2105.12791.
- [18] J.-T. Lee, D. Bollegala, and S. Luo, ““touching to see” and “seeing to feel”: Robotic cross-modal sensory data generation for visual-tactile perception,” in *2019 International Conference on Robotics and Automation (ICRA)*, IEEE, 2019, pp. 4276–4282.
- [19] M. A. Lee, Y. Zhu, K. P. Srinivasan, P. Shah, S. Savarese, L. Fei-Fei, A. Garg, and J. Bohg, “Making sense of vision and touch: Self-supervised learning of multimodal representations for contact-rich tasks,” *2019 International Conference on Robotics and Automation (ICRA)*, pp. 8943–8950, 2019.
- [20] Y. Li, J.-Y. Zhu, R. Tedrake, and A. Torralba, “Connecting touch and vision via cross-modal prediction,” in *Proceedings of the IEEE/CVF Conference on Computer Vision and Pattern Recognition*, 2019, pp. 10 609–10 618.
- [21] J. Lin, R. Calandra, and S. Levine, “Learning to identify object instances by touch: Tactile recognition via multimodal matching,” in *2019 International Conference on Robotics and Automation (ICRA)*, IEEE, 2019, pp. 3644–3650.
- [22] Y. Lu, J. Wang, and V. Kumar, “Curiosity driven self-supervised tactile exploration of unknown objects,” *arXiv preprint arXiv:2204.00035*, 2022.
- [23] S. Luo, W. Yuan, E. Adelson, A. G. Cohn, and R. Fuentes, “Vitac: Feature sharing between vision and tactile sensing for cloth texture recognition,” in *2018 IEEE International Conference on Robotics and Automation (ICRA)*, IEEE, 2018, pp. 2722–2727.
- [24] B. Mildenhall, P. P. Srinivasan, M. Tancik, J. T. Barron, R. Ramamoorthi, and R. Ng, “Nerf: Representing scenes as neural radiance fields for view synthesis,” in *European Conference on Computer Vision (ECCV)*, 2020.
- [25] M. A. Mousa, M. Soliman, M. A. Saleh, and A. G. Radwan, “Tactile sensing biohybrid soft e-skin based on bioimpedance using aloe vera pulp tissues,” *Scientific Reports*, vol. 11, no. 3054, 2021.
- [26] C. Pacchierotti, S. Sinclair, M. Solazzi, A. Frisoli, V. Hayward, and D. Prattichizzo, “Wearable haptic systems for the fingertip and the hand: Taxonomy, review, and perspectives,” *IEEE Transactions on Haptics*, vol. 10, no. 4, pp. 580–600, 2017.
- [27] L. Pecyna, S. Dong, and S. Luo, “Visual-tactile multimodality for following deformable linear objects using reinforcement learning,” *ArXiv*, vol. abs/2204.00117, 2022.
- [28] A. Radford, J. W. Kim, C. Hallacy, A. Ramesh, G. Goh, S. Agarwal, G. Sastry, A. Askell, P. Mishkin, J. Clark, G. Krueger, and I. Sutskever, “Learning transferable visual models from natural language supervision,” in *International Conference on Machine Learning (ICML)*, 2021.
- [29] O. Russakovsky, J. Deng, H. Su, J. Krause, S. Satheesh, S. Ma, Z. Huang, A. Karpathy, A. Khosla, M. Bernstein, A. C. Berg, and L. Fei-Fei, “ImageNet Large Scale Visual Recognition Challenge,” *International Journal of Computer Vision (IJCV)*, vol. 115, no. 3, pp. 211–252, 2015.
- [30] E. P. Scilingo, N. Sgambelluri, and A. Bicchi, “The role of tactile flow in processing dynamic haptic stimuli,” in *The Sense of Touch and its Rendering: Progress in Haptics Research*, A. Bicchi, M. Buss, M. O. Ernst, and A. Peer, Eds. Berlin, Heidelberg: Springer Berlin Heidelberg, 2008, pp. 39–60.
- [31] D. Seita, A. Ganapathi, R. Hoque, M. Hwang, E. Cen, A. K. Tanwani, A. Balakrishna, B. Thananjeyan, J. Ichnowski, N. Jamali, K. Yamane, S. Iba, J. F. Canny, and K. Goldberg, “Deep imitation learning of sequential fabric smoothing from an algorithmic supervisor,” *2020 IEEE/RSJ International Conference on Intelligent Robots and Systems (IROS)*, pp. 9651–9658, 2020.
- [32] Y. She, S. Wang, S. Dong, N. Sunil, A. Rodriguez, and E. H. Adelson, “Cable manipulation with a tactile-reactive gripper,” *The International Journal of Robotics Research*, vol. 40, pp. 1385–1401, 2020.
- [33] L. Smith and M. Gasser, “The development of embodied cognition: Six lessons from babies,” *Artificial Life*, vol. 11, pp. 13–29, 2005.
- [34] N. Sunil, S. Wang, Y. She, E. Adelson, and A. R. Garcia, “Visuotactile affordances for cloth manipulation with local control,” in *Conference on Robot Learning (CoRL)*, 2022.
- [35] S. Suresh, Z. Si, S. Anderson, M. Kaess, and M. Mukadam, “Midastouch: Monte-carlo inference over distributions across sliding touch,” in *Conference on Robot Learning (CoRL)*, 2022.
- [36] K. Takahashi and J. Tan, “Deep visuo-tactile learning: Estimation of tactile properties from images,” in *2019 International Conference on Robotics and Automation (ICRA)*, IEEE, 2019, pp. 8951–8957.
- [37] Z. Wu, Y. Xiong, S. X. Yu, and D. Lin, “Unsupervised feature learning via non-parametric instance-level discrimination,” *CoRR*, vol. abs/1805.01978, 2018. arXiv: 1805.01978.
- [38] W. Yuan, S. Wang, S. Dong, and E. Adelson, “Connecting look and feel: Associating the visual and tactile properties of physical

- materials,” in *Proceedings of the IEEE Conference on Computer Vision and Pattern Recognition*, 2017, pp. 5580–5588.
- [39] M. Zambelli, Y. Aytar, F. Visin, Y. Zhou, and R. Hadsell, “Learning rich touch representations through cross-modal self-supervision,” in *Conference on Robot Learning (CoRL)*, 2020.
- [40] W. Zheng, H. Liu, and F. Sun, “Lifelong visual-tactile cross-modal learning for robotic material perception,” *IEEE Transactions on Neural Networks and Learning Systems*, vol. 32, no. 3, pp. 1192–1203, 2021.
- [41] S. Zhong, A. Albini, O. P. Jones, P. Maiolino, and I. Posner, “Touching a nerf: Leveraging neural radiance fields for tactile sensory data generation,” in *Conference on Robot Learning (CoRL)*, 2022.